Thermal Transport in Nanoporous Silicon: Interplay between Disorder at Mesoscopic and Atomic Scales

Yuping He, Davide Donadio, Joo-Hyoung Lee,[§] Jeffrey C. Grossman,[§] and Giulia Galli*

[†]Department of Chemistry and [‡]Department of Physics, University of California, Davis, California 95616, United States and [§]Department of Material Science and Engineering, Massachusetts Institute of Technology, Cambridge, Massachusetts 02139, United States

ABSTRACT We present molecular and lattice dynamics calculations of the thermal conductivity of nanoporous silicon, and we show that it may attain values 10−20 times smaller than in bulk Si for porosities and surface-to-volume ratios similar to those obtained in recently fabricated nanomeshes. Further reduction of almost an order of magnitude is obtained in thin films with thickness of 20 nm, in agreement with experiment. We show that the presence of pores has two main effects on heat carriers: appearance of non-propagating, diffusive modes and reduction of the group velocity of propagating modes. The former effect is enhanced by the presence of disorder at the pore surfaces, while the latter is enhanced by decreasing film thickness.

KEYWORDS: thermal conductivity · silicon nanoporous materials · molecular dynamics

Thermoelectric materials,[1,2] which can both generate electricity from waste heat and use electricity for solid-state Peltier cooling,[3] are to date inefficient, compared to conventional generators and refrigerators.[4] The efficiency of a thermoelectric material is expressed by a dimensionless figure of merit, ZT, defined as $ZT = S^2\sigma T/\kappa$, where S is the Seebeck coefficient, σ and κ are the electrical and thermal conductivity, respectively, and T is the temperature. One way to obtain systems with improved efficiency is to engineer nanostructured semiconductors,[5−7] so as to reduce κ of the crystalline materials while preserving their electronic properties. Such a strategy has been recently applied to silicon, an earth-abundant, cheap, and non-toxic material. Crystalline Si (c-Si) is not a good thermal-to-electrical energy converter, with ZT = 0.01[8] and $\kappa \approx 150$ W/mK at room temperature.[9,10] However, at the nanoscale, Si thermoelectric properties can be greatly improved: Si wires have been fabricated[11,12] with κ up to 100 times smaller than that of c-Si and ZT ≈ 0.6. The thermal conductivities of nanomeshes[13] and porous membranes[14] have been made even smaller than those of nanowires for specific choices of the pore size and spacing, without degrading the electronic properties of c-Si.

Even though both the thermal conductivity reduction reported experimentally and the preservation of bulk Si electronic properties have been predicted by atomistic[15] and electronic structure[16] calculations, the microscopic origin of the reduction of κ in nanoporous silicon (np-Si) has not yet been investigated and remains poorly understood. In addition, the surface-to-volume ratio studied theoretically[15,16] was higher than that obtained experimentally, and only bulk samples were considered, and thus surface effects were neglected (while recent nanomeshes have been built out of thin films).

In this paper we report molecular and lattice dynamics calculations of the thermal conductivity of np-Si, and we establish the role of and the interplay between several effects contributing to thermal transport, including film thickness, porosity, surface-to-volume ratio, and the presence of amorphous surface layers. We consider np-Si with porosity similar to that of recently fabricated nanomeshes,[13] and we find that the presence of nanometer-sized holes may lead to values of κ that are 10 to 20 times smaller than in c-Si, depending on the degree of order at their surfaces. Additional reduction of about 1 order of magnitude is obtained in thin (20 nm) nanoporous films, in agreement with experiment.[13] We also find that, by combining mesoscopic- (presence of pores) and atomic-scale disorder at surfaces, one may engineer a nanostructured Si material with much reduced thermal conductivity in both the directions perpendicular and parallel to the pores.

* Address correspondence to gagalli@ucdavis.edu.

Received for review October 5, 2010 and accepted January 31, 2011.

Published online February 10, 2011
10.1021/nn2003184

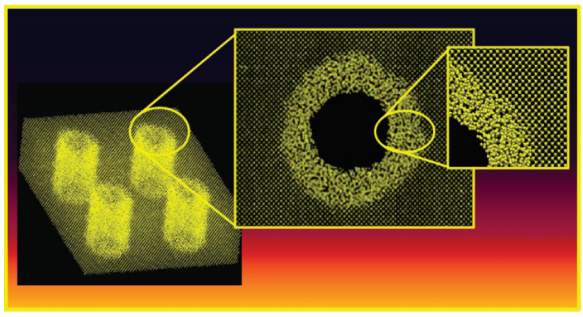

Figure 1. Representative microscopic picture of nanoporous materials investigated in the present work. We studied samples with both ordered and disordered surfaces, as indicated by the insets, and both bulk systems and thin films.

RESULTS AND DISCUSSION

Figure 1 gives a pictorial representation of the np-Si samples studied here, which have been chosen with porosities similar to those of recent experiments. We first conducted a series of molecular dynamics (MD) simulations with the empirical potential proposed by Tersoff[17] on bulk samples, and we investigated the effects on the value of the thermal conductivity, of atomistic disorder at pore surfaces, and of pore misalignment. We then simulated thin films to investigate the effect of sample size reduction, and finally thin films with pores. After establishing a series of results with MD simulations, we used lattice dynamics calculations to analyze and interpret our data. In particular, we computed several properties of the heat carriers identified in the simulated systems, including their propagating character, mean free paths, and lifetimes. Lattice dynamics calculations are essential to provide insights into the modification of the properties of the heat carriers on going from bulk to np-Si and into their dependence on porosity, film thickness, and surface morphology and disorder. (Details of our calculations are given both in the Computational Details section and in the Supporting Information.) Finally, our results were used to interpret experiments.

MD Simulations for Bulk Samples. We start by discussing our MD results. We define porosity and surface-to-volume ratio of np-Si as $\phi = \pi d_p^2/(2d_p + 2d_s)^2$ and $\rho = \pi d_p/(d_p + d_s)^2$, where d_s and d_p are pore spacing and diameter, respectively. We denote by κ_c and κ_{np} the thermal conductivity of crystalline and nanoporous Si, respectively. Table 1 shows our computed values of κ_c/κ_{np} for bulk np-Si samples with $\phi = 0.07$ (and pores in the 100 direction) as a function of ρ. The values of ϕ and ρ for the nanomeshes studied experimentally[13] are 0.08 and 0.16 1/nm, respectively. We find that the ratio κ_c/κ_{np} decreases as a function of ρ; even for relatively small values of ρ (0.07 1/nm), κ_{np} of np-Si with ordered surfaces (OS) is 7 times smaller than that of the bulk. In the range $\rho = 0.16-0.07$ 1/nm, the dependence of κ_{np} on ρ appears to be weak.

If atomistic disorder is present at the pore surfaces, the thermal conductivity of np-Si further decreases with respect to that of the crystal: we obtain a ratio κ_c/κ_{np} of about 20 in the presence of disordered surfaces (DS) for $\rho = 0.07$ 1/nm (see third column of Table 1), instead of 7 as in the case of ordered surfaces. In our simulations, disorder at pore surfaces was obtained by heating an ordered sample to 2800 K and then cooling it to 300 K while allowing a small region close to the surface to amorphize. The DS of the samples shown in the third column of Table 1 contain 18% noncrystalline sites, and disorder was characterized with an order parameter typically adopted for tetrahedrally bonded materials.[18,19] Increasing the disorder from 18 to 26% (corresponding to six and eight disordered atomic layers, respectively) lowers κ by approximately 20 to 30%. We note that, for $\rho = 0.071$/nm, the computed ratio κ_c/κ_{np}(DS) (~20) is consistent with the value reported in ref 14 for the Si membranes with the smallest hole radius (the ratio is ~25); however, a direct comparison is not straightforward, as in ref 14 $\phi \approx 0.1$, $\rho \approx 0.01$ 1/nm, and the thickness of the DS is about 1−2 nm. It is also interesting to note that, in the case of samples with disordered surfaces, the thermal conductivity in the direction parallel (as opposed to perpendicular) to the pores is also greatly decreased, by at least a factor of 10 compared to the corresponding systems with ordered surfaces.

TABLE 1. Ratio between thermal conductivity computed for bulk crystalline Si and for nanoporous Si in the plane perpendicular to the pores, with ordered surfaces (OS) and disordered surfaces (DS), as a function of the surface-to-volume ratio (ρ) for a sample with porosity $\phi = 0.07$[a]

ρ (1/nm)	κ_c/κ_{np}(OS)	κ_c/κ_{np}(DS)	d_s (nm)	d_p (nm)
0.3	28	68	2.3	1
0.16	12	34	4.4	2.3
0.07	7	19	10	4.4
0.07 *mis.*	10		10	4.4

[a] The porosity was chosen to be similar to that of recently fabricated nanomeshes. For each sample, we also give the distance between pores (d_s) and the pore diameter (d_p). "*mis.*" denotes a sample with misaligned pores.

Since experimental samples are likely to exhibit a certain degree of misalignment between pores, for the system with the lowest value of ρ, we carried out a simulation with misaligned pores. We considered four pores per unit cell, yielding a total of 86 576 atoms. Three of the pores are aligned, and one is misaligned

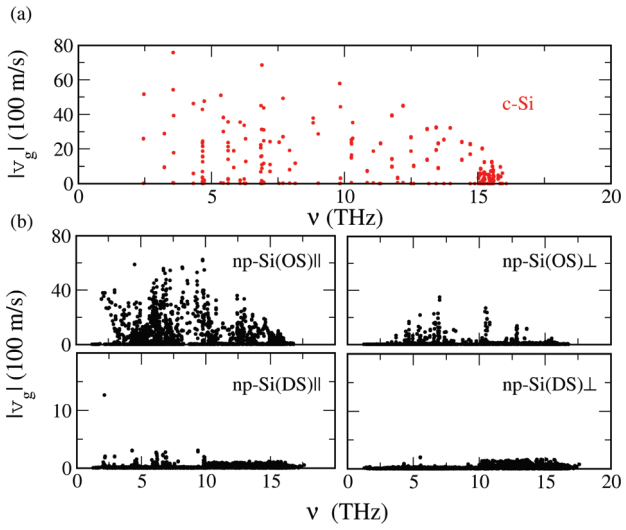

Figure 2. (a) Group velocity as a function of frequency for c-Si. (b) Group velocity as a function of frequency for np-Si with ordered [np-Si(OS)] and disordered [np-Si(DS)] surfaces (the two samples have the same porosity, $\phi = 0.07$). The left and right panels show the group velocity in the direction parallel to the pores and in the direction perpendicular to the pores, respectively.

by 2 nm in both the *x* and *y* directions. As expected, having slightly misaligned pores further decreases κ by another 30% (see Table 1).

MD Simulations for Thin Films. We now turn to discuss our MD data obtained for thin films. We first evaluated the reduction of κ with respect to that of the bulk in a 20 nm crystalline homogeneous thin film (no pores). We considered two cases: one film with smooth, reconstructed 2×1 surfaces and one with 1 nm rough surfaces, to mimic experimental samples, which are prepared as Si on oxide and are expected to have a thin oxide layer at their surfaces. We found a reduction by a factor of 3 and 7, respectively; this result is consistent with experiment,[13] where the ratio $\kappa_c/\kappa_{\text{thin-film}} \approx 7.5$. Finally, we simulated a 20 nm thin film with the same porosity as the bulk samples discussed above ($\phi = 0.07$) and a surface-to-volume ratio close to experiment ($\rho =$ 0.07 1/nm). In this case we considered only ordered pore surfaces and smooth thin-film surfaces, and we found a reduction by a factor of 3 with respect to a crystalline thin-film sample (no pores) of the exact same thickness. The reduction found experimentally is larger (close to 9); however, we note that including the effects of pore misalignment and disordered pore surfaces brings our results very close to the experimental ones.[13]

Lattice Dynamics Calculations and Interpretation of MD Data. In order to characterize, at the microscopic scale, the properties of the heat carriers of np-Si, and to understand how they differ from those of c-Si, we carried out a series of lattice dynamics calculations. We focused on a specific system ($\phi = 0.07$ and $\rho = 0.3$ 1/nm), and we first considered a sample with ordered surfaces [np-Si(OS)]. We find that, in this system, due to the presence of pores, the group velocities v_g of acoustic modes below 3−5 THz in the direction perpendicular to the pores are greatly decreased with respect to those in c-Si (most of them by approximately 1 order of magnitude) (see Figure 2). This change greatly contributes to the decrease of thermal conductivity in the direction perpendicular to the pores found in our MD simulations. In contrast, we observe a very moderate decrease of v_g in the direction parallel to the pores, consistent with the small decrease of thermal conductivity in this direction (of the order of 10%) with respect to that of c-Si. The speed of sound in the sample is reduced by approximately 10% with respect to the crystalline bulk in both the longitudinal and transverse directions. In addition, an analysis of the polarization of vibrational modes shows that, in our np-Si samples, a considerable amount of vibrations are no longer propagating but rather become diffusive, as in amorphous silicon (a-Si).[20,21] An analysis of the spatial extent of the eigenvectors of the dynamical matrix corresponding to diffusive modes, or diffusons (not shown), shows a polynomial rather than an exponential decay as a function of distance, similar to what is found in a-Si.[21] Therefore, diffusons do not exhibit an Anderson localization-type behavior, but possibly a weak localization of the Ioffe Regel type.[22] Due to their spatial extent, diffusive modes overlap with each other and thus are heat carriers, although they are much less effective than phonons. The relative contributions of diffusive and propagating modes to the thermal conductivity of np-Si can be evaluated by describing phonons with the Boltzman transport equation in the single-mode relaxation time approximation and by describing diffusive modes using the theory devised in ref 20. Such an approach has been recently applied to vibrations of core−shell Si nanowires.[23,24] We find that about 25% of the thermal conductivity (2.4 W/mK) of our np-Si sample originates from propagating modes with reduced group velocities with respect to

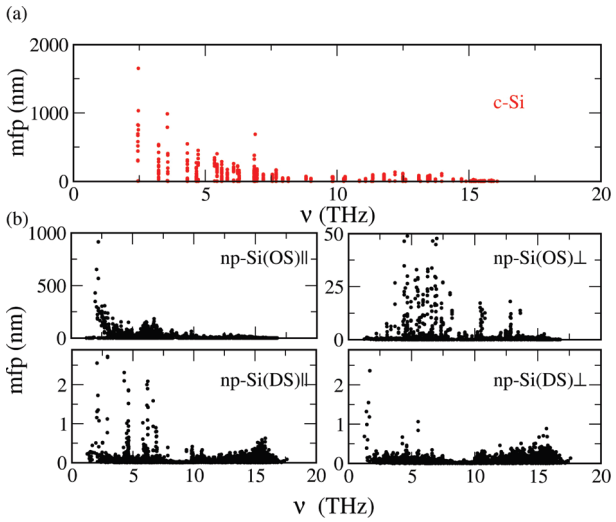

Figure 3. (a) Mean free path as a function of frequency for c-Si. (b) Mean free path as a function of frequency for the same np-Si samples shown in Figure 2. The left and right panels show the mean free path in the direction parallel to the pores and in the direction perpendicular to the pores, respectively.

c-Si, and the rest (8 W/mK) comes from diffusive modes. The sum of the two contributions yields a value in agreement with that computed independently in our MD simulations (10 ± 0.2 W/mK). The mean free paths of low-frequency, propagating modes of [np-Si(OS)] attain values up to 50 nm in the direction perpendicular to the pores and of the order of a micrometer in the direction parallel to the pores (see Figure 3).

Next we carried out lattice dynamics calculations for np-Si with disordered surfaces [np-Si(DS)]. Our results show that amorphization of the pore surfaces leads to an increased density of diffusive modes. Effective group velocities decrease both in the directions parallel and perpendicular to the pores. While group velocities of vibrational modes are greatly affected by both mesoscopic (*i.e.*, presence of pores) and atomistic disorder, lifetimes (τ, not shown) exhibit a less dramatic variation. The existence of nanoscale pores only leads to a moderate decrease of τ (by a factor of 2−3, depending on porosity) with respect to the crystal. It is the presence of amorphized surfaces that considerably lowers the lifetimes, especially the ones of low-frequency modes.

CONCLUSIONS

In summary, our results show that the presence of pores in np-Si samples has two main effects on heat carriers: (i) appearance of non-propagating, diffusive modes and (ii) reduction of the group velocity of propagating modes (phonons). The relative proportions of diffusive and propagating modes depend on pore spacing and distance; for example, in the sample with $\phi = 0.07$ and $\rho = 0.3$ 1/nm, we find that 25% of the thermal conductivity is accounted for by phonons and the rest by so-called diffusons. As ρ increases, the phonon contribution is expected to decrease. The extent to which the group velocity (and thus the mean free path) of low-frequency propagating modes is reduced with respect to the bulk depends again on pore size and spacing. We find that effect (i) is enhanced by the presence of disorder at the pore surfaces; *i.e.*, at fixed ϕ and ρ, the proportion of diffusive modes increases in np-Si with disordered surfaces, and thus κ decreases. Effect (ii) is enhanced by decreasing film thickness. Overall, our findings are consistent with those obtained for two- and three-dimensional model porous system (*e.g.*, Lennard-Jones Ar)[25] and for nonporous thin films.[26] Work is in progress to investigate how alloying effects may further decrease the thermal conductivity of group IV nanoporous materials, building on promising results we have obtained for SiGe thin wires.[27]

COMPUTATIONAL DETAILS

We carried out equilibrium MD simulations in the NVE (constant number of particles N, volume V, and energy E) ensemble and computed κ from the fluctuations of the heat current, using the Green−Kubo relation based on the fluctuation, dissipation theorem: $\kappa_\alpha = 1/k_B V T^2 \int_0^{t_{max}} \langle J_\alpha(t) J_\alpha(0) \rangle \, dt$, where k_B is the Boltzmann constant, V is the volume of the system, T is the temperature, and $\langle J_\alpha(t) J_\alpha(0) \rangle$ is the average of the autocorrelation function of the heat current (J) along the α direction, given by $J_\alpha(t) = d/dt \sum_i r_{i\alpha}(t) \varepsilon_i(t)$. Here ε_i is the energy density associated with atom i, with position r. Interatomic forces were described using the empirical potential proposed by Tersoff.[17] Although this potential is known to overestimate the melting T of crystalline Si, it is a useful tool to study trends of

the thermal conductivity as a function of, *e.g.*, T and nanostructuring and to analyze the nature of vibrational modes in Si-based materials. The computed κ of c-Si (279 ± 26 W/mK at 300 K) is overestimated with respect to experiment (150−200 W/mK at room temperature[9,10]). The computed speed of sound (∼6347 m/s) is overestimated as well (the experimental value is 5639 m/s). Table 1S summarizes all the systems simulated in this work. Convergence tests as a function of simulation time for np-Si are given in Figure 1S, and convergence tests as a function of size for both np-Si and c-Si are reported in Figures 2S and 3S, respectively.

In lattice dynamic calculations, the dynamical matrix Ω was obtained by computing derivatives of forces acting on atoms as finite differences. Ω was computed and diagonalized (to obtain eigenvectors e and eigenvalues ω) at the Γ point ($\vec{q} = 0$) of the supercell Brillouin zone and for several small, finite $\vec{q}$-points: $\Omega_{ij}(\vec{q}) = \Omega_{ij}(\vec{q} = 0)e^{i\vec{q}\cdot\vec{r}_{ij}}$, where $\vec{r}_{ij} = \vec{r}_i - \vec{r}_j$ and $\vec{r}$ denotes atomic positions. For a disordered system, the group velocities $\vec{v}_{\vec{q}=0} = d\omega/d\vec{q}$ at the Γ-point are zero, except for the three acoustic modes corresponding to $\omega = 0$. However, in the case of np-Si, dispersion curves show that low-frequency modes retain propagating character and $\omega(q)$ flattens out only for $\vec{q} \approx 0$. We therefore define an effective group velocity as $\vec{v}_{\vec{q}=0} = \Delta\omega/\Delta\vec{q}$, without taking the limit for $q \to 0$. (We considered 20 q values spaced by 0.002 A^{-1} over an interval of 0.04 A^{-1} excluding the Γ-point, and we approximated dispersion curves by a quadratic function obtained by least-squares fit.) For non-propagating, diffusive modes, $v_{\vec{q}} \approx 0$. Lifetimes were computed from the normalized autocorrelation function of the energy of the eigenmodes:

$$\tau_i = \int_0^\infty \frac{\langle E_i(\vec{q},t)E_i(\vec{q},0)\rangle}{\langle E_i(\vec{q},0)E_i(\vec{q},0)\rangle}dt$$

where

$$E_i(\vec{q},t) = \frac{\omega_i^2 S_i^*(\vec{q},t)S_i(\vec{q},t)}{2} + \frac{S_i^{'*}(\vec{q},t)S_i'(\vec{q},t)}{2}$$

$$S_i(\vec{q},t) = \sqrt{N}\sum_j \sqrt{M_j}\, e^{(-i\vec{q}\cdot\vec{r}_{j,0})}\, e_i^*(\vec{q})\cdot u_j(t)$$

S' is the time derivative of S, and u_j is the displacement of atom j in our MD trajectories. In the case of bulk Si, we computed the thermal conductivity from lattice dynamics data using the Boltzmann transport equation (non-self-consistent solution in the single-mode relaxation time approximation): $\kappa = \sum_i c_i v_i^2 \tau_i$. The sum extends to all modes, and c_i is the specific heat per unit volume of mode i. We obtained a value of 266 W/mK, in agreement with our MD results (279 ± 26 W/mK). In the case of np-Si, both propagating ($v_{\vec{q}\neq 0}$) and non-propagating, diffusive modes ($v_{\vec{q}\approx 0}$) contribute to heat transport; following our work on Si nanowires, we decomposed κ as $\kappa = \sum_i c_i v_i^2 \tau_i + \sum_j c_j D_j$, where the sum over i extends to all propagating modes and that over j to all diffusive modes. $D_{j\alpha} = (V^2/8\pi^2\hbar^2\nu_j^2)\cdot\sum_{k\neq j}|\langle e_j|J_\alpha|e_k\rangle|^2\,\delta(\nu_j - \nu_k)$, where $\langle e_j|J_\alpha|e_k\rangle$ is the α component of the heat flux operator projected on eigenvectors e_j and e_k. The decomposition into diffusive and propagating modes is done using a cutoff on the group velocities. We show in Figure 4S that, while in c-Si the value of κ is fully accounted for by propagating modes, only 25% of κ in np-Si is accounted for by propagating modes.

Acknowledgment. Y.H., D.D. and G.G. gratefully acknowledge support from DOE/BES grant no. DE-FG02-06ER46262. J.C.G. and J.-H.L. are grateful for support from the Defense Threat Reduction Agency-Joint Science and Technology Office for Chemical and Biological Defense (Grant HDTRA1-09-10006). We thank Slobodan Mitrovic and Ivana Savic for useful discussions.

Supporting Information Available: Details of system size and morphology, MD simulation time, and convergence tests as a function of simulation time for np-Si and as a function of size for both np-Si and c-Si. This material is available free of change *via* the Internet at http://pubs.acs.org.

REFERENCES AND NOTES

1. Snyder, G. J.; Toberer, E. S. Complex Thermoelectric Materials. *Nat. Mater.* **2008,** *7*, 105–114.
2. Minnich, A. J.; Dresselhaus, M. S.; Ren, Z. F.; Chen, G. Bulk Nanostructured Thermoelectric Materials: Current Research and Future Prospects. *Energy Environ. Sci.* **2009,** *2*, 466–479.
3. Chowdhury, I.; Prasher, R.; Lofgreen, K.; Chrysler, G.; Narasimhan, S.; Mahajan, R.; Koester, D.; Alley, R.; Venkatasubramanian, R. On-Chip Cooling by Superlattice-Based Thin-Film Thermoelectrics. *Nature Nanotechnol.* **2009,** *4*, 235–238.
4. Vining, C. B. An Inconvenient Truth about Thermoelectrics. *Nat. Mater.* **2009,** *8*, 83–85.
5. Venkatasubramanian, R.; Siivola, E.; Colpitts, T.; O'Quinn, B. Thin-Film Thermoelectric Devices with High Room-Temperature Figures of Merit. *Nature* **2001,** *413*, 597–602.
6. Hsu, K. F.; Loo, S.; Guo, F.; Chen, W.; Dyck, J. S.; Uher, C.; Hogan, T.; Polychroniadis, E. K.; Kanatzidis, M. G. Cubic AgPbmSbTe2+m: Bulk Thermoelectric Materials with High Figure of Merit. *Science* **2004,** *303*, 818–821.
7. Poudel, B.; Hao, Q.; Ma, Y.; Lan, Y.; Minnich, A.; Yu, B.; Yan, X.; Wang, D.; Muto, A.; Vashaee, D..; *et al.* High-Thermoelectric Performance of Nanostructured Bismuth Antimony Telluride Bulk Alloys. *Science* **2008,** *320*, 634–638.
8. Rowe, D. M., *CRC Handbook of Thermoelectrics*; CRC-Press: Boca Raton, FL, 1995; p 701.
9. Capinski, W. S.; Maris, H. J.; Bauser, E.; Silier, I.; Asen-Palmer, M.; Ruf, T.; Cardona, M.; Gmelin, E. Thermal Conductivity of Isotopically Enriched Si. *Appl. Phys. Lett.* **1997,** *71*, 2109–2111.
10. Kremer, R. K.; Graf, K.; Cardona, M.; Devyatykh, G. G.; Gusev, A. V.; Gibin, A. M.; Inyushkin, A. V.; Taldenkov, A. N.; Pohl, H. J. Thermal Conductivity of Isotopically Enriched 28Si: Revisited. *Solid State Commun.* **2004,** *131*, 499–503.
11. Hochbaum, A. I.; Chen, R. K.; Delgado, R. D.; Liang, W. J.; Garnett, E. C.; Najarian, M.; Majumdar, A.; Yang, P. D. Enhanced Thermoelectric Performance of Rough Silicon Nanowires. *Nature* **2008,** *451*, 163–167.
12. Boukai, A. I.; Bunimovich, Y.; Tahir-Kheli, J.; Yu, J. K.; Goddard, W. A.; Heath, J. R. Silicon Nanowires as Efficient Thermoelectric Materials. *Nature* **2008,** *451*, 168–171.
13. Yu, J.-K.; Mitrovic, S.; Tham, D.; Varghese, J.; Heath, J. R. Reduction of Thermal Conductivity in Phononic Nanomesh Structures. *Nature Nanotechnol.* **2010,** *5*, 718–721.
14. Tang, J.; Wang, H.-T.; Lee, D. H.; Fardy, M.; Huo, Z.; Russell, T. P.; Yang, P. Holey Silicon as an Efficient Thermoelectric Material. *Nano Lett.* **2010,** *10*, 4279–4283.
15. Lee, J. H.; Grossman, J. C.; Reed, J.; Galli, G. Lattice Thermal Conductivity of Nanoporous Si: Molecular Dynamics Study. *Appl. Phys. Lett.* **2007,** *91*, 223110.
16. Lee, J.-H.; Galli, G. A.; Grossman, J. C. Nanoporous Si as an Efficient Thermoelectric Material. *Nano Lett.* **2008,** *8*, 3750–3754.
17. Tersoff, J. Modeling Solid-State Chemistry—Interatomic Potentials for Multicomponent Systems. *Phys. Rev. B* **1989,** *39*, 5566–5568.
18. Steinhardt, P. J.; Nelson, D. R.; Ronchetti, M. Bond-Orientational Order in Liquids and Glasses. *Phys. Rev. B* **1983,** *28*, 784–805.
19. Li, T.; Donadio, D.; Galli, G. Nucleation of tetrahedral solids: a Molecular Dynamics Study of Supercooled Liquid Silicon. *J. Chem. Phys.* **2009,** *131*, 224–519.
20. Allen, P. B.; Feldman, J. L. Thermal-Conductivity of Disordered Harmonic Solids. *Phys. Rev. B* **1993,** *48*, 12581–12588.
21. Allen, P. B.; Feldman, J. L.; Fabian, J.; Wooten, F. Diffusons, Locons and Propagons: Character of Atomic Vibrations in Amorphous Si. *Philos. Mag. B* **1999,** *79*, 1715–1731.
22. Taraskin, S. N.; Elliott, S. R. Determination of the Ioffe-Regel Limit for Vibrational Excitations in Disordered Materials. *Philos. Mag. B* **1999,** *79*, 1747–1754.
23. Donadio, D.; Galli, G. Atomistic Simulations of Heat Transport in Silicon Nanowires. *Phys. Rev. Lett.* **2009,** *102*, 195–901.

24. Donadio, D.; Galli, G. Temperature Dependence of the Thermal Conductivity of Thin Silicon Nanowires. *Nano Lett.* **2010,** *10*, 847–851.
25. Lukes, J. R.; Tien, C. L. Molecular Dynamics Simulation of Thermal Conduction in Nanoporous Thin Films. *Microscale Therm. Eng.* **2004,** *8*, 341–359.
26. Turney, J. E.; McGaughey, A. J. H.; Amon, C. H. In-Plane Phonon Transport in Thin Films. *J. Appl. Phys.* **2010,** *107*, 024317.
27. Chan, M. K. Y.; Reed, J.; Donadio, D.; Mueller, T.; Meng, Y. S.; Galli, G.; Ceder, G. Cluster Expansion and Optimization of Thermal Conductivity in SiGe Nanowires. *Phys. Rev. B* **2010,** *81*, 303–303.